Establishment of a human skeletal muscle-derived cell line: biochemical, cellular and electrophysiological characterization.

Ori Rokach[*], Nina D. Ullrich[†], Martin Rausch[‡], Vincent Mouly[§], Haiyan Zhou[ll], Francesco Muntoni[5], Francesco Zorzato[*,¶±] and Susan Treves[*,¶±]

[*]Departments of Anaesthesia and Biomedicine, University Hospital Basel, Hebelstrasse 20, 4031 Basel, Switzerland; [†]Department of Physiology, University of Bern, Bern, Switzerland; [‡]Novartis Biomedical Institute, Postfach 4002 Basel, Switzerland; [§]Thérapie des maladies du muscle strié, Institut de Myologie, UM76, UPMC, Université Paris 6, Paris, France; [ll]Dubowitz Neuromuscular Centre, Institute of Child Health, University College London WC1N 1EH, UK; [¶]Department of Life Sciences and Biotechnology, University of Ferrara, Ferrara, Italy.

Short title: *Characterization of a human skeletal muscle cell line*

To whom correspondence should be addressed: Susan Treves, Departments of Anaesthesia and Biomedicine, Basel University Hospital, Hebelstrasse 20, 4031 Basel, Switzerland. Tel. +41-61-2652373; Fax:+41-61-2653702; E-mail: susan.treves@unibas.ch or Francesco Zorzato, Departments of Life Sciences, University of Ferrara, Ferrara, Italy. Tel. +39-0532-455-356; E-mail: zor@unife.it.
[±]both authors contributed equally.

Key words: immortalized muscle cells, excitation-contraction coupling, super resolution microscopy, gene expression.

SYNOPSIS

Excitation contraction coupling is the physiological mechanism occurring in muscle cells whereby an electrical signal sensed by the dihydropyridine receptor located on the transverse tubules is transformed into a chemical gradient (Ca^{2+} increase) by activation of the ryanodine receptor located on the sarcoplasmic reticulum membrane. In the present investigation we characterized for the first time the excitation contraction coupling machinery of an immortalized human skeletal muscle cell line. Intracellular Ca^{2+} measurements showed a normal response to pharmacological activation of the ryanodine receptor whereas super resolution structured illumination microscopy (3D-SIM) revealed a low level of structural organization of ryanodine receptors and dihydropyridine receptors. Interestingly, the expression levels of several transcripts of proteins involved in calcium homeostasis and differentiation indicate that the cell line has a phenotype closer to that of slow twitch than fast twitch muscles. These results point to the potential application of such human muscle-derived cell lines to the study of neuromuscular disorders; in addition they may serve as a platform for the development of therapeutic strategies aimed at correcting defects in calcium homeostasis due to mutations in genes involved in calcium regulation**.**

INTRODUCTION

Skeletal muscle is a highly differentiated tissue made up of myofibers, a syncytium of cells filled with myofibrils and containing sarcomeres that generate the force necessary for muscle contraction. During the past few years a number of techniques have been developed to isolated single muscle fibers from small rodents allowing detailed investigations of the functional properties of the excitation contraction (EC) coupling mechanism at the ultrastructural, biochemical and cellular levels in normal and pathological conditions [1-4]. Because of their high degree of differentiation and specialization, it is difficult to maintain differentiated muscle fibers in culture for more than a few days [5] and it is nearly impossible to obtain mature fibers starting from precursor satellite cells. Nevertheless, starting from newborn mice one can obtain cultures of contracting and striated myotubes that can be used for a number of manipulations. As to human muscle cells, primary cultures can be obtained *in vitro* by culturing satellite cells from biopsies and differentiating them into myotubes [6-9], but there is a clear necessity to develop cell lines from control and diseased individuals which will develop into myotubes and which can be exploited as a platform for drug screening, and for biochemical, cellular and physiological characterization [10-13].

For the past two decades our laboratory as well as others, have established primary cultures from human biopsies and characterized their intracellular Ca^{2+} homeostasis, with particular emphasis on EC coupling, how endogenous mutations in the ryanodine receptor Ca^{2+} channel (RyR1) affect its functional properties and some downstream effects of calcium dysregulation such as subcellular localization of the transcription factor NFAT, pro-inflammatory cytokine release and production of reactive nitrogen species [9,14,15]. However, the use of primary cultures has some inherent drawbacks mainly relating to the fact that they are generally slow growing and will undergo a limited number of divisions. To overcome this problem, immortalization of human myogenic cells has recently been established both from a normal individual [16,17] as well as from patients with different neuromuscular diseases [17-20]. In the present study we characterized a new cell line derived from a normal individual with no overt neuromuscular disorder. We show that the myotubes derived upon differentiation by serum withdrawal express the transcripts and protein components of the skeletal muscle EC coupling machinery. In addition, we established by super resolution structured illumination microscopy (3D-SIM) the subcellular distribution of the RyR1 and of the dihydropyridine receptor and assessed calcium release via RyR by using optical and electrophysiological techniques. This human skeletal muscle cell line HMCL-7304 is a tool of paramount importance to study on a larger scale the changes occurring in human muscles under a variety of pathological conditions.

EXPERIMENTAL PROCEDURES

Cell culture: The immortalized myoblast cell line was established from the intercostals skeletal muscle biopsy of a 19-year-old female donor with no neuromuscular disorder by double transfection with recombinant retroviruses containing the telomerase (hTERT) cDNA and Cdk4 cDNA, as previously described [16,17]. Immortalized myoblasts were maintained in skeletal muscle cell growth medium (PromoCell GmbH, Heidelberg, Germany; catalogue N° c-23060) in low oxygen atmosphere (5% O_2 and 5% CO_2) at 37º C. In order to induce differentiation, once the density had reached approximately 80%, cells were rinsed one time with Phosphate Buffered Saline (PBS, pH 7.2; Life Technologies, Lucerne, Switzerland) and incubated with skeletal muscle differentiation medium (PromoCell GmbH, Heidelberg, Germany; catalogue N° c-23061). The process of differentiation took on average 5 days after which multinucleated myotubes were clearly visible under low magnification. Henceforward the Human Muscle derived-Cell Line will be referred to as HMCL-7304.

[Ca^{2+}] Measurements: HMCL-7304 cells were grown and differentiated on glass cover slips coated with laminin (10µg/ml; Life Technologies, Lucerne, Switzerland). Once myotubes had formed, cells were loaded with the fluorescent Ca^{2+} indicator Fluo-4/AM (Life Technologies, Lucerne, Switzerland) for 40 minutes at 37 °C as previously described [15]. Cells were rinsed one time with Krebs-Ringer containing 2 mM $CaCl_2$ and then coverslips were mounted onto a 37ºC thermostated chamber which was continuously perfused with Krebs Ringer medium; individual cells were stimulated with the indicated agonists (KCl, 4-chloro-*m*-cresol, caffeine) made up in Krebs Ringer containing no added Ca^{2+} plus 100 µM La^{3+} in order to monitor changes in the cytoplasmic calcium concentration due to release from intracellular stores. Individual cells were stimulated by means of an 8-way 100mm diameter quartz micromanifold computer-controlled microperfuser (ALA Scientific Instruments, Farmingdale, New York, U.S.A.), as previously described [14]. On-line fluorescence images were acquired using an inverted Nikon TE2000 TIRF microscope equipped with a dry Plan Apochromat 20x objective (N.A. 0.17) and an electron multiplier Hamamatsu CCD camera C9100-13. Changes in the free cytosolic calcium concentration were analyzed using MetaMorph (Molecular Devices) imaging system and the average pixel value for each cell was measured as previously described [14,15].

Electrophysiological measurements and confocal Ca^{2+} imaging: Myoblasts were grown on laminin-coated glass-bottom 35 mm dishes (MatTek). After differentiation into myotubes, cells were patch-clamped in the whole-cell configuration with low-resistance borosilicate glass micropipettes (1-3 MΩ) using an Axopatch 200B amplifier (Axon Instruments, Union City, CA) controlled by a custom-written data-acquisition software developed by LantibodiesView (National Instruments, Austin, TX). The external solution contained (in mM): 150 TEA-CH_3SO_3, 2 $CaCl_2$, 1 $MgCl_2$, 10 HEPES, 0.001 TTX, 1 4-AP, pH was adjusted to 7.4 with CsOH. The pipette solution contained (in mM): 140 Cs-CH_3SO_3, 10 HEPES, 6 $MgCl_2$, 11.5 $CaCl_2$, 4 Na_2ATP, 20 EGTA, 14 $CrPO_4$, 0.1 Leupeptin, 0.1 K_5-Fluo-3, pH was adjusted to 7.2 with CsOH (21). The reference electrode was connected to the bath solution with an agar bridge (4% agar in 3 M KCl). All measurements were done at room temperature. Holding potential was kept at –80 mV. Step-wise depolarizations were applied to activate the voltage-dependent dihydropyridine receptor (DHPR) and to trigger Ca^{2+} release mediated by the ryanodine receptor (RyR1), the intracellular Ca^{2+}-release channel located in the sarcoplasmatic reticulum (SR)

membrane. Detailed voltage-clamp protocols are indicated. In order to determine the current-voltage relationship, long depolarizations of 800 ms were applied. Currents were analyzed in IgorPro (Wavemetrics, Lake Oswego, OR). Peak current amplitude was calculated from the difference between membrane currents before and during application of 500 mM $CdCl_2$ (ΔI_{CaL}). For the investigations of electromechanical coupling between DHPR and RyR1, short depolarizations (50 ms) were applied. Changes in intracellular Ca^{2+} levels $[Ca^{2+}]_i$ were monitored using the fluorescent Ca^{2+} indicator fluo-3 (Biotium), which was loaded into the cell via the patch pipette. Using a laser-scanning confocal microscope (MicroRadiance, Biorad, Hercules, CA), fluo-3 was excited at 488 nm with an argon ion laser, and emission light was collected above 500 nm. Linescan images were recorded at a rate of 50 lines/sec, analyzed in ImageSXM (free software based on NIH Image) [22] and further processed using IgorPro. Changes in $[Ca^{2+}]_i$ are shown as relative changes in fluorescence ($\Delta F/F_0$).

qPCR experiments: Total RNA was extracted from differentiated HMCL-7304 myotubes and biopsies from healthy individuals, using Trizol (Life Technologies, Lucerne, Switzerland) as previously described [23]. cDNA was synthesized with the High Capacity cDNA synthesis kit (Applied Biosystem) and the following primers: ***RYR1*** **(**Forward : 5' -ATC TCC CGC CTT AGC CAT ACT TCT -3' and Reverse: 5' -GGA CCT CTA CGC CCT GTA TC- 3'); ***RYR3*** (Forward 5'-CAG TCC CTA TCT GTC AGA GCC -3' and Reverse 5'- CAT GGC CGT ATA ACA GGG TCC -3') ; ***CAV 1.1*** (Forward: 5'-ACG AAC ATG CAC CTA GCC AC- 3' and Reverse 5'- ACG AAC ATG CAC CTA GCC AC- 3') ; ***CASQ 1*** (Forward**:** 5'-CAC CCA AGT CAG GGG TAC AG- 3' and Reverse: 5'-GTG CCA GCA CCT CAT ACT TCT- 3') ; ***CASQ 2*** (Forward 5'-CAT TGC CAT CCC CAA CAA ACC -3' and Reverse 5'-AGA GTG GGT CTT TGG TGT TCC -3'); ***DES 1*** **(**Forward 5' -AAC CAG GAG TTT CTG ACC ACG -3' and Reverse: 5'- TTG AGC CGG TTC ACT TCG G -3'); ***MYH 1*** (Forward 5'- GGG AGA CCT AAA ATT GGC TCA A -3' and Reverse 5'- TTG CAG ACC GCT CAT TTC AAA -3'); ***MYH 2*** (Forward 5'- AGA AAC TTC GCA TGG ACC TAG -3' and Reverse 5'- CCA AGT GCC TGT TCA TCT TCA -3'); ***SERCA 1*** (Forward 5'-GGT GCT GGC TGA CGA CAA CT -3' and Reverse 5'-AAG AGC CAG CCA CTG ATG AG -3'); ***SERCA 2*** (Forward 5'-CTC CAT CTG CCT GTC CAT-3' and Reverse 5'-GGC TGA CGG CTT CCA AGT-3'). Transcript levels were quantified using Syber Green reagent on an Applied Biosystems platform (7500 fast real time PCR system) and levels were normalized to Desmin expression.

Mouse muscle fiber isolation: Mouse *flexor digitorum brevis* (FDB) fibers were enzymatically dissociated at 37°C for 60 min in a cell culture incubator in Tyrode's solution containing 0.20% collagenase I (Sigma Fine Chemicals, St. Louis, M.O., U.S.A.; catalogue N° C0130-16) and placed on glass coverslips previously coated with 1.5 µl laminin (1 mg/ml) (catalogue N° 23017-015; Life Technologies, Lucerne, Switzerland) as previously described [23].

Immunofluorescence: For immunofluorescence, myotubes cultured on glass coverslips were fixed with 4% paraformaldehyde at room temperature for 15 min, washed and permeabilized with 0.1% Triton-PBS for one hour before blocking with 3% goat serum for 30 min, followed by one hour incubation in mouse anti-fast myosin monoclonal antibody (1:100; Sigma Fine Chemicals, St. Louis, M.O., U.S.A.; catalogue N° M4276) and mouse anti-slow myosin monoclonal antibody (1:50; Novo NCL, Leica Biosystem, Newcastle, UK, catalogue N° NCL-MHC) at room temperature. Coverslips were washed in 0.1% Triton-PBS and incubated with

goat-anti-mouse secondary antibody conjugated to Alexa Fluor 594 (Life Technologies, Lucerne, Switzerland, catalogue N° A-11005), for one hour at room temperature, followed by thorough washing in PBS. Nuclei were stained with Hoechst 33258 (Invitrogen, catalogue N° H3569) for 10 min. Slides were mounted in aqueous mounting medium and viewed with a Leica DMR fluorescent microscope equipped with a 20x HC-PL Fluotar objective (N.A.0.50). The percentage of fast and slow myosin positive HMCL-7304-derived myotubes was calculated by counting the number of myosin positive cells divided by the total numbers of cells as visualized by brightfield microscopy in the same area. For super resolution microscopy, FDB fibers or human skeletal muscle myotubes were fixed with 3.7% paraformaldehyde (in PBS) for 30 min at room temperature, rinsed 2 x with PBS and permeabilized with 1% Triton-X 100 in PBS for 30 min. After rinsing and blocking non specific sites with 1:100 Roche blocking solution, cells and fibers were incubated with the following antibodies for 3 hours at room temperature (final concentration 10 µg/ml diluted in PBS+ 0.01% Tween): mAb anti-RyR1 (Thermo Scientific, Catalogue N° MA3-925), goat anti- $Ca_v1.s$ (Santa Cruz, catalogue N° sc-8160). Slides were rinsed with PBS-T 5 times 5 min each and incubated with the appropriate secondary conjugate (Alexa Fluor 555; Alexa Fluor 647, Life Technologies, Lucerne, Switzerland, 1:500 diluted in PBS-T) over night at 4°C. Slides were rinsed with PBS-T and mounted with 10% glycerol in PBS. Staining was visualized with a Zeiss Elyra microscope equipped with 63X oil Plan-Apochromat (1.4 N.A.) objective. Raw data sets consisted of images acquired with three different grid angles and 5 different grid phases. Super resolution images were calculated from the raw data using the build-in algorithm. The baseline was just shifted (not truncated) to allow inspection for potential ghosts arising from sample imperfections.

Electrophoresis and immunoblotting: Microsomes were prepared from differentiated HMCL-7304 derived myotubes as previously described [24]. Protein concentration was determined using the BioRad kit (catalogue N° 500-0006) using bovine serum albumin as a standard. SDS-PAGE, protein transfer onto nitrocellulose and immunostaining were performed as previously described [24]. The following primary antibodies were used: mouse anti-RyR1 (Thermo Scientific, MA3-925), rabbit anti-RyR1 (a kind gift of Prof. V. Sorrentino), goat anti-$Ca_v1.1$ (Santa Cruz, catalogue N° sc-8160), rabbit anti-CASQ1 (Sigma, catalogue N° CO743), rabbit anti-CASQ2 (Epitomics, catalogue N° 29621), goat anti-SERCA1 (Santa Cruz catalogue N° sc-8093), goat anti-SERCA2 (Santa Cruz catalogue N° sc-8095), mouse anti-MYH1 (Millipore catalogue N° MAB S1628). Secondary peroxidase-conjugates were Protein-G POD (Sigma catalogue N° 8170) and anti-mouse POD (Sigma catalogue N° 2304). The immunopositive bands were visualized by chemiluminescence using the Super Signal West Dura kit (Thermo Scientific).

Statistical analysis and graphic software: Statistical analysis was performed using the Student's *t* test; means were considered statistically significant when the P value was <0.05. When more than two groups were compared, analysis was performed by the ANOVA test followed by the Bonferroni post hoc test using Graphpad Prism 4.0 software. The Origin software was used to generate dose response curves and obtain EC_{50} values; images were assembled using Adobe Photoshop CS Version 8.0.

RESULTS

Expression levels of proteins involved in excitation-contraction coupling in cell line-derived myotubes.

In order to functionally characterize the HMCL-7304 –derived myotubes, we chose several genes that are well known to play a crucial role in skeletal muscle EC coupling. Transcript levels were quantified and compared to those present in muscle biopsies obtained from five healthy individuals. Figure 1A shows the relative expression levels on a logarithmic scale, of different transcripts. Interestingly, we found that the *RYR1* transcript was significantly lower (approximately 300 times) compared to differentiated muscle ($P<0.0001$), and there was no up-regulation of *RYR3* mRNA, which was also significantly reduced in HMCL-7304 myotubes. *SERCA1* and *CSQ1* transcript levels were significantly lower (≈1000 times) in the cell line ($P<0.003$), whereas there was a 10-fold increase in the expression of the *CSQ2* transcript. *SERCA2* showed similar mRNA levels in the biopsies and the cell line as did $Ca_v1.1$, suggesting that expression of the L-type Ca^{2+} channel may appear at an early stage of development. The transcript level of myosin heavy chain 1 (*MYH1*) and myosin heavy chain2 (*MYH2*), that are characteristically expressed in slow twitch and fast twitch muscles respectively, were lower in HMCL-7304 compared to biopsies however, immunofluorescence shows that the slow myosin isoform is present in a larger percentage of HMCL-7304 cells, compared to fast myosin, with a ratio of approximate 51% (slow) to 13% (fast) (36% negative for both fast and slow isoforms) (Fig.1 B). Taken together these results suggest that the differentiated myotubes express proteins that are more abundant in slow twitch muscles.

We are aware that the presence of a transcript does not necessarily reflect protein expression, thus we tested microsomes prepared from HMCL-7304-derived myotubes by immunoblotting. Figure 1C confirms that MYH1, SERCA1, SERCA2, $Ca_v1.1$ and RyR1 were all expressed. The double immunopositive band seen in the RyR1 western blot does not represent RyR3 since both bands were present when a RyR1 specific polyclonal antibody was used; thus the lower band is probably a degradation product. No bands were visualized when blots were probed with anti-CSQ1 antibodies (not shown) but a band migrating with an approximate molecular mass of 55 kDa (asterisk) was present when myotube microsomes were probed with anti-CSQ2 antibodies.

Cellular localization of EC coupling proteins:

In mature skeletal muscle, EC coupling occurs and is fully dependent on the architecture of highly structured intracellular calcium release units, whereby the voltage sensing L-type Ca^{2+} channel is present in the transverse tubules and faces the terminal cisternae of the sarcoplasmic reticulum, containing the RyR1 Ca^{2+} release channels. The sarcoplasmic reticulum contains the calcium binding protein calsequestrin, whereas the SERCA Ca^{2+} pumps are located on the longitudinal sarcoplasmic reticulum. In order to define the cellular localization of these proteins in mature myotubes, we used a super resolution (Structured Illumination Microscopy, 3D-SIM) microscope, because compared to conventional confocal fluorescence microscopy and Stimulated Emission Depletion microscopy it offers improved lateral (approx. 100 nm) and axial resolution (approx. 300 nm) [25]. Figure 2 shows the immunostaining of $Ca_v1.1$ and RyR1 both in myotubes (A-F) and in enzymatically dissociated mouse FDB fibers (G-I). As expected in FDB fibers the staining with anti-$Ca_v1.1$ shows a double row of fluorescent particles (Fig. 2G) that mostly overlap with particles which are stained with anti-RyR1 antibodies (Fig. 2H). Human

myotubes also show fluorescent particles whose distribution does not follow the highly regular pattern observed in mature FDB fibers. However, when observed at high magnification it becomes apparent that human myotubes display areas containing multiple parallel longitudinal rows of fluorescence particles which are stained anti-$Ca_v1.1$ antibodies (Fig. 2D double arrows). A large fraction of particles stained with anti-$Ca_v1.1$ antibodies co-localize with particles stained with anti-RyR1 antibodies (Fig. 2F arrowheads) and may represent calcium release units involved in EC coupling. In the next set of experiments, we assessed the EC coupling characteristics of HMCL-7304-derived myotubes, by studying RyR- mediated Ca^{2+} release and $Ca_v1.1$ mediated Ca^{2+} currents either by optical methods or by using the patch-clamp technique in the whole-cell configuration.

Functional properties and pharmacological activation of calcium release:

Figure 3 shows the results obtained in cells loaded with the fluorescent Ca^{2+} indicator fluo-4; stimulation of cells with 60 mM KCl caused an immediate increase in the resting [Ca^{2+}] which decayed back to resting values within approximately 5 seconds (Fig 3B); the peak increase in [Ca^{2+}] was similar irrespective of whether cells were stimulated via activation of the DHPR L-type Ca^{2+} channel by KCl-induced depolarization, or by direct activation of the RyR1 with 4-chloro-m-cresol and caffeine (Fig. 3 C). Panels 3D, E and F show dose dependent peak Ca^{2+} release curves elicited by caffeine, 4-chloro-m-cresol and KCl respectively as well as the calculated EC_{50} values. These results are similar to those obtained in primary human muscle myotubes explanted from biopsies from control individuals [14,15].

We then investigated the voltage-dependence of membrane currents (I_{CaL}) from the DHPR in voltage-clamped HMCL-7304 myotubes. Starting from a holding potential of –80 and an initial pre-step to –40 mV, cells were stimulated by repetitive depolarizing steps of 800 ms in 10 mV increments to increasing membrane potentials. Figure 4A shows 5 steps of the stimulation protocol (upper trace) and the corresponding membrane currents (below) during control conditions (black) and during inhibition of I_{CaL} with Cd^{2+} (red). The calculated difference current (ΔI_{CaL}) is indicated in blue and peak current amplitudes at the end of the depolarizing steps are used for further analysis. Figure 4B summarizes the voltage-dependence of current activation and reveals a half-maximal activation ($V_{1/2}$) at –9 mV.

A parallel investigation of electromechanical coupling was achieved using a combination of voltage-clamp and confocal Ca^{2+} imaging. Cells were imaged in the linescan mode at close proximity to the position of the patch pipette. Membrane depolarization triggered significant Ca^{2+} release, indicating functional coupling between the DHPR and RyR1. Depolarization-induced Ca^{2+} release was monitored and recorded in linescan images. Figure 5A shows a voltage-clamped HMCL-7304 myotube loaded with fluo-3; the position of the linescan is indicated in the illustrated myotube. Short depolarization (50 ms) starting from the holding potential of -80 mV to +10 mV activated the DHPR and triggered Ca^{2+} release from the SR. The resulting Ca^{2+} transient is displayed in the linescan image and in the corresponding line profile. Of note is the slow return of the [Ca^{2+}] back to resting levels, which might be a consistent with low level of SERCA1 expression in immature myotubes (see Figure 1A). As expected, increasing membrane depolarization results in greater Ca^{2+} release, which saturates at a membrane potential of around 0 mV. Figure 5B shows the Ca^{2+} transient amplitude in response to increasing depolarization in a single protocol, and Figure 5C summarizes the voltage-dependence of Ca^{2+} release. In order to minimize side effects from long periods of scanning and accumulation of cytosolic Ca^{2+} due to slow Ca^{2+} extrusion processes, data points for peak Ca^{2+}

transients in Figure 5C have been collected from repeated short linescan recordings (6 sec). Ca^{2+} transients elicited under voltage clamp revealed a half-maximal release activation ($V_{1/2}$) at –32 mV.

DISCUSSION

In the present manuscript we describe the biochemical, cellular and physiological characteristics of a novel cell line generated from human skeletal muscle. The necessity to establish cell lines of human origin from normal or patients affected by a number of neuromuscular conditions has been apparent for the past decades but early attempts to immortalize human myoblasts capable of differentiating into mature myotubes were unsuccessful (for example see ref. [26 and 27]). Here, we report the successful myotube differentiation from myoblasts of the newly generated immortal human muscle cell line HMCL-7304 derived from a healthy individual and characterize their features at the biochemical, structural and functional level, showing that their phenotype is similar to myotubes from primary cultures.

In the past few years a number of groups have exploited vectors expressing telomerase- and cyclin-dependent kinase 4 and have reported successful immortalization of myoblasts from normal individuals and individuals affected by various forms of muscular dystrophies and dysferlinopathies [16-20]. The possibility of generating such immortalized cell lines able to differentiate into myotubes constitutes an important tool to investigate human neuromuscular diseases much like the murine skeletal muscle C_2C_{12} cell line has been exploited during the past decades by laboratories worldwide to investigate key aspects of skeletal muscle physiology and plasticity. Therefore, there is high demand for a reliable human skeletal cell line to fill the gap between understanding the pathophysiological mechanisms and the development of therapeutic strategies for human neuromuscular disorders. Nevertheless, though the use of an immortalized cell line has many advantages over primary cultures, the process of immortalization is known to modify many physiological parameters ranging from differentiation and secretion, to the expression of specific protein isoforms. For this reason we characterized the EC coupling machinery and Ca^{2+} homeostasis of HMCL-7304-derived myotubes. We chose to verify the levels of expression of the transcripts encoding the main components of skeletal muscle EC coupling, as well as their main isoforms and compared them to the levels found in biopsies from human skeletal muscle fibers from normal individuals. Transcripts encoding RyR1, calsequestrin 1 and SERCA1 were significantly down regulated as was RyR3, an isoform that is thought to be more abundantly expressed in developing muscles. On the other hand, $Ca_V1.1$ was expressed to similar levels in both mature fibers and myotubes and produced large Ca^{2+} currents, as shown in patch clamp measurements. These results are in contrast to what occurs during skeletal muscle development, where components of the sarcoplasmic reticulum appear at an earlier stage of development compared to the transverse-tubules containing the dihydropyridine receptor L-type Ca^{2+} channel [29-31]. Interestingly, the relative mRNA expression of HMCL-7304 derived myotubes was either similar to that of mature biopsies (SERCA2) or upregulated (calsequestrin 2). Thus it seems that the HMCL-7304 cell line has more the characteristics of a “slow twitch” than that of a “fast twitch” muscle. This is further confirmed by the predominant expression of slow myosin compared to fast myosin in differentiated HMCL-7304 myotubes. Several reasons may explain this observation: (i) either satellite stem cells are by default “slow-twitch-like” and it is the influence of innervation or electrical activity that enables them to become fast or slow [32], (ii) the immortalization procedure “selects” satellite stem cells that have a “slow muscle” phenotype, (iii) as reported in hindlimb muscles of adult rats, the satellite cells contained within fast or slow twitch fibers are intrinsically different subpopulations [33] so that the HMCL-7304 cell line that originated from dorsal muscles resembles more a slow-twitch muscle from which it originated.

Two noticeable differences in the physiological characteristics of human cultured myotubes and mature fibers are that primary myotubes do not contract and the time scale of the depolarization-induced Ca^{2+} transient occurs in hundreds of milliseconds in myotubes while it lasts only a few millseconds in mature fibers. While the lack of contracture most likely reflects the composition of the actomyosin contractile machinery, the slow calcium transients observed in myotubes probably reflects the lower level of expression of SERCA1 and the absence of a highly organized micro-architecture. After Ca^{2+} release, cytosolic Ca^{2+} is rapidly removed and pumped back into the SR lumen by the SR Ca^{2+} ATPase (SERCA), which is the main protein of non-junctional SR in skeletal muscle fibers [34]. Reduced SERCA1 expression levels as shown in HMCL-7304 cell line have a significant impact on the Ca^{2+} removal kinetics leading to deceleration of Ca^{2+} re-uptake compared to normal muscle fibers. Thus, lack of mature subcellular architectural organization and reduction in SERCA1 expression may explain the slow Ca^{2+} removal after release in the HMCL-7304 cell line.

In mature fibers four $Ca_v1.1$ on the T-tubular face in square formation, referred to as tetrads, are directly opposite the four subunits of one RyR1 tetramer on the sarcoplasmic reticulum junctional membrane, to form the calcium release units [30]. In intact FDB fibers the calcium release units form double rows on each side of the Z line. The highly organized arrangement is characteristic of mature skeletal muscle and is probably one of the features allowing the extremely rapid Ca^{2+} release kinetics upon T tubules membrane depolarization. As evidenced by the SIM images, HMCL-7304 myotubes show distinct rows of $Ca_v1.1$ that overlap at least in part, with RyR1 and we believe that these structures may represent the calcium release units of the HMCL-7304 myotubes. This conclusion is consistent with whole patch clamp measurements showing that voltage-induced Ca^{2+} release is highly functional in these myotubes, indicating direct coupling between sarcolemmal DHPRs and RyR1 despite structural immaturity. HMCL-7304 myotubes exhibit Cd^{2+}-sensitive Ca^{2+} currents, having half-maximal current activation at -9 mV, a value which is comparable to that published by others [35, 36]. Parallel imaging revealed that the voltage dependence of Ca^{2+} release ($V_{1/2}$) was -32 mV in the present report and -29.4 mV in non-immortalized primary human myotubes from control individuals [37], which is similar to the values (-26 mV) obtained on primary myotubes from wild type mice [38]. Furthermore, the process of immortalization do not affect the pharmacological characteristics of RyR1 activation since the caffeine and 4-chloro-m-cresol dose response curves of the HMCL-7304 cell line are similar to those of non-immortalized human myotubes [14, 39] or RyR1 isolated from mature rodent muscles [40].

In conclusion in this study we characterized a human muscle cell line derived from a normal individual and show that it retains a pattern of expression of proteins involved in EC coupling similar to that of slow twitch muscles. The ability to perform pharmacological and electrophysiological studies illustrates the potential use of such a biological tool to a variety of approaches from studying the effect of mutations and gene silencing to testing drugs and pharmacological agents aimed at correcting calcium dysregulation as occurs in a variety of neuromuscular disorders including core myopathies.

ACKNOWLEDGEMENTS
We would like to thank Prof. Vincenzo Sorrentino, University of Siena for kindly providing the polyclonal rabbit anti- RyR1 antibody. The support of the MRC Neuromuscular Centre and the GOSH Biomedical Research Centre to the Biobank is gratefully acknowledged. This work was supported by the SNF (grant N° 3100 030_129785) to ST; SNF-Ambizione PZ00P3_131987 to N.D.U.; Muscular Dystrophy Association grant to FM (grant N° 174047) and a grant from the Botnar Stiftung. The supports of the MDA USA MDA68762 grant to FM and the platform for immortalization of human cells from the Myologie Institute in Paris are also gratefully acknowledged. FM is supported by the Great Ormond Street Children's Charity.

ABBREVIATIONS
$Ca_v1.1$, alfa 1 subunit of the dihydropyridine receptor; CSQ, calsequestrin; DHPR, dihydropyridine receptor; EC coupling, excitation contraction coupling; FDB, flexor digitorum brevis; HLMC-1, human muscle derived-cell line; MYH, myosin heavy chain; PBS, phosphate buffered saline; RyR, ryanodine receptor; SERCA, sarco(endo)plasmic reticulum ATPase; SIM, structured illumination microscopy; SR, sarcoplasmic reticulum.

REFERENCES

1. Ravenscroft, G., Nowak, K.J., Jackaman, C., Clément, S., Lyons, M.A., Gallagher, S., Bakker, A.J. and Laing, N.G. (2007) Dissociated flexor digitorum brevis myofiber culture system-a more mature muscle culture system. Cell. Motil. Cytoskeleton **64**, 727-738
2. Calderon, J.C., Bolaños, P., Torres, S.H., Rodríguez-Arroyo, G. and Caputo, C.J. (2009) Different fibre populations distinguished by their calcium transient characteristics in enzymatically dissociated murine flexor digitorum brevis and soleus muscles. Muscle Res. Cell Motil. **30**, 125-137
3. Calderon, J.C., Bolaños, P. and Caputo, C. (2011). Kinetic changes in tetanic Ca^{2+} transients in enzymatically dissociated muscle fibres under repetitive stimulation. J. Physiol. **589**, 5269-5283
4. Lovering, R.M., Michaelson, L. and Ward, C.W. (2009) Malformed *mdx* myofibers have normal cytoskeletal architecture yet altered EC coupling and stress-induced Ca^{2+} signaling. Am. J. Physiol. Cell. Physiol. **297**, C571-C580
5. Brown, L.D., Rodney, G.G., Hernàdez-Ochoa, E. and Schneider, M.F. (2007) Ca^{2+} sparks and T-tubule reorganization in dedifferentiating adult mouse skeletal muscle fibers. Am. J. Physiol. Cell. Physiol. **292**, C1156-C1166
6. Yasin, R., Van Beers, G., Nurse, K.C., Al-Ani, S., Landon D.N. and Thompson, E.J. (1977) A quantitative technique for growing human adult skeletal muscle in culture starting from mononucleated cells. J. Neurol. Sci. **32**,347–359
7. Zuurveld, J.G.E.M., Oosterhof, A., Veerkamp, J.H. and van Moerkerk, H.T.B. (1985). Oxidative metabolism of cultured human skeletal muscle cells in comparison with biopsy material. Biochim. Biophys. Acta. **844**, 1–8
8. Blau, H.M. and Webster, C. (1981) Isolation and characterization of human muscle cells. Proc. Natl. Acad. Sci. USA. **78**, 5623–5627
9. Censier, K, Urwyler, A., Zorzato, F. and Treves, S. (1991) Intracellular calcium homeostasis in human primary muscle cells from malignant hyperthermia-susceptible and normal individuals. Effect Of overexpression of recombinant wild-type and Arg163Cys mutated ryanodine receptors. J. Clin. Invest. **15**, 1233-1242
10. Yaffe, D. and Saxel, O. (1977) Serial passaging and differentiation of myogenic cells isolated from dystrophic mouse muscle. Nature **270**, 725-727
11. Lorenzon, P., Grohovaz, F. and Ruzzier, F. (2000) Voltage- and ligand-gated ryanodine receptors are functionally separated in developing C2C12 mouse myotubes. J. Physiol. **525**, 499-507
12. McMahon, D.k., Anderson, P.A., Nassar, R., Bunting, J.B., Saba, Z., Oakeley, A.E. and Malouf NN. (1994) C2C12 cells: biophysical, biochemical, and immunocytochemical properties. Am. J. Physiol. Cell Physiol. **266**, C1795-C1802
13. Gutierrez-Martin, Y., Martin-Romero, F.J. and Henao, F. (2005) Store operated calcium entry in differentiated C2C12 skeletal muscle cells. Biochim. Biophys. Acta. **1711**, 33-40
14. Ducreux, S., Zorzato, F., Muller, C., Sewry, C., Muntoni, F., Quinlivan, R., Restagno, G., Giraird, T. and Treves, S. (2004). Effect of ryanodine receptor mutations on interleukin-6 release and intracellular calcium homeostasis in human myotubes from malignant hyperthermia-susceptible individuals and patients affected by central core disease. J. Biol. Chem. **279**, 43838-43846

15. Treves, S., Vukcevic, M., Jeannet, P.Y., Levano, S., Girard, T., Urwyler, A., Fischer, D., Voit, T., Jungbluth, H., Lillis, S., Muntoni, F., Quinlivan, R., Sarkozy, A., Bushby, K. and Zorzato F. (2010) Enhanced excitation-coupled Ca^{2+} entry induces nuclear translocation of NFAT and contributes to IL-6 release from myotubes from patients with central core disease. Hum. Mol. Genet. **20**, 589-600
16. Zhu, C.H., Mouly, V., Cooper, R.N., Mamchaoui, K., Bigot, A., Shay, J.W., Di Santo J.P., Butler-Browne, G.S. and Wright W.E. (2007) Cellular senescence in human myoblasts is overcome by human telomerase reverse transcriptase and cyclin-dependent kinase 4: consequences in aging muscle and therapeutic strategies for muscular dystrophies. Aging cell **6**, 515-523
17. Mamchaoui, K., Trollet, C., Bigot, A., Negroni, E., Chaouch, S., Wolff, A., Kandalla, P.K., Marie, S., Di, S.J., St Guily, J.L., Muntoni, F., Kim, J., Philippi, S., Spuler, S., Levy, N., Blumen, S.C., Voit, T., Wright, W.E., Aamiri, A., Butler-Browne, G. and Mouly, V. (2011) Immortalized pathological human myoblasts: towards a universal tool for the study of neuromuscular disorders. Skelet. Muscle **1**,1-34
18. Hashimoto, N., Kiyono, T., Wada, M.R., Shimizu, S., Yasumoto, S. and Ingagawa, M. (2005). Immortalization of human myogenic progenitor cell clone retaining multipotentiality. Biochem. Biophys. Res. Commun. **348**, 1383-1388
19. Shiomi, K., Kiyono, T., Okamura, K., Uezumi, M., Goto, Y., Yasumoto, S., Shimizu, S and Hashimoto, N: (2011) CDK4 and cyclin D1 allow human myogenic cells to recapture growth property without compromising differentiation potential. Gene Therapy **18**, 857-866
20. Philippi, S., Bigot, A., Marg, A., Mouly, V., Spuler, S. and Zacharias, U. (2012). Dysferlin-deficient immortalized human myoblasts and myotubes as a useful tool to study dysferlinopathy. PLoS. Curr. Doi: 10.1371/currents. RRN1298
21. Prosser, B.L., Hernandez-Ochoa, E.O., Zimmer, D.B. and Schneider, M.F. (2009) The Qgamma component of intra-membrane charge movement is present in mammalian muscle fibres, but suppressed in the absence of S100A1. J. Physiol. **587**, 4543-4559
22. Barrett, S.D. (2002) Software for scanning microscopy. Proc. R. Microsc. Soc. **37**, 167-174
23. Mosca, B., Delbono, O., Messi, L.M., Bergamelli, L., Wang, Z.M., Vukcevic, M., Lopez, R., Treves, S., Nishi, M., Takeshima, H., Paolini, C., Martini, M., Rispoli, G., Protasi, F. and Zorzato, F. (2013) Enhanced dihydropyridine receptor calcium channel activity restores muscle strength in JP45/CASQ1 double knockout mice. Nat. Commun. **4**,1541. doi:10.1038/ncomms2496
24. Anderson, A.A., Treves,S., Biral, D., Betto, R., Sandonà, D., Ronjat, M. and Zorzato, F. (2003) The novel skeletal muscle sarcoplasmic reticulum JP-45 protein. Molecular cloning, tissue distribution, developmental expression, and interaction with alpha 1.1 subunit of the voltage-gated calcium channel. *J. Biol. Chem*. **278**, 39987-39992
25. Schermelleh, L., Heintzmann, R. and Leonhardt H. (2010) A guide to super-resolution fluorescence microscopy. J. Cell Biol. **190**, 777-791
26. DeCaprio, J.A., Ludlow, J.W., Figge, J., Shew, J.Y., Huang, C.M., Lee, W.H., Marsilio, E., Paucha, E. and Livingston, D.M. (1988) SV40 large tumor antigen forms a specific complex with the product of the retinoblastoma susceptibility gene. Cell **54**, 275–283
27. Simon, L.V., Beauchamp, J.R., O'Hare, M. and Olsen, I. (1996) Establishment of long-term myogenic cultures from patients with Duchenne muscular dystrophy by retroviral

transduction of a temperature-sensitive SV40 large T antigen. Exp. Cell Res. **224**, 264-271
28. Zhou, H., Rokach, O., Feng, L., Munteanu, I., Mamchaoui, K., Wilmhurst, J.M., Sewry, C., Manzur, A.Y., Pillay, K., Mouly, V., Duchen, M., Jungbluth, H., Treves, S. and Muntoni, F. (2013) RyR1 deficiency in congenital myopathies disrupts excitation-contraction coupling. Hum. Mutat. doi: 10.1002/humu.22326
29. Franzini-Armstrong, C. and Jorgensen, A.O. (1994) Structure and development of E–C coupling units in skeletal muscle. Annu. Rev. Physiol. **56**, 509–534
30. Flucher, B.E., Andrews, S.B., Fleischer, S., Marks, A.R., Caswell, A. and Powell, J.A. (1993) Triad formation: organization and function of the sarcoplasmic reticulum calcium release channel and triadin in normal and dysgenic muscle in vitro. J. Cell Biol. **123**, 1161-1174
31. Al-Qusari, L. and Laporte, J. (2011) T-tubule biogenesis and triad formation in skeletal muscle and implication in human diseases. Skelet. Muscle **26,** doi: 10.1186/2044-5040-1-26
32. Nedachi, T., Fujita, H. and Kanzaki, M. (2008) Contractile C2C12 myotube model for studying exercise-inducible responses in skeletal muscle. Am. J. Physiol. Endocrinol. Metab. **295**, E1191-E1204
33. Kalhovde, J.M., Jerkovic, R., Sefland, I., Cordonnier, C., Calantibodiesria, E., Schiaffino. S. and Lømo, T. (2005) "Fast" and "slow" muscle fibres in hindlimb muscles of adult rats regenerate from intrinsically different satellite cells. J. Physiol. **562**, 847-857
34. Periasamy, M. and Kalyanasundaram, A. (2007) SERCA pump isoforms:their role in calcium transport and disease. Muscle Nerve **35**, 430-442
35. Delbono, O. (1992). Calcium current activation and charge movement in denervated mammalian skeletal muscle fibres. J. Physiol. **451**, 187-203
36. Hernandez-Ochoa, E.O. and Schneider, M.F. (2012) Voltage clamp methods for the study of membrane currents and SR Ca release in adult skeletal muscle fibers. Prog. Biophys. Mol. Biol. **108**, 98-118
37. Ullrich ND, Fischer D, Kornblum C, Walter MC, Niggli E, Zorzato F, Treves S. (2011) Alterations of excitation-contraction coupling and excitation coupled Ca^{2+} entry in human myotubes carrying CAV3 mutations linked to rippling muscle. Hum. Mutat. **32**, 309-317
38. Chelu, M.G., Goonasekera, S.A., Durham, W.J., Tang, W., Lueck, J.D., Riehl, J., Pessah, I.N., Zhang, P., Bhattacharjee, M.B., Dirksen, R.T. and Hamilton, S.L. (2006) Heat- and anesthesia-induced malignant hyperthermia in an RyR1 knock-in mouse FASEB. J. **20**, 329-330
39. Kaufmann, A., Kraft, B., Michalek-Sauberer, A., Weindlmayr, M., Kress, H.G., Steinboeck, F. and Weigl, L.G. (2012) Novel double and single ryanodine receptor 1 variants in two Austrian malignant hyperthermia families. Anesth. Analg. **114**,1017-25
40. Zorzato, F., Scutari, E., Tegazzin, V., Clementi, E. and Treves, S. (1993) Chlorocresol: an activator of ryanodine receptor-mediated Ca^{2+} release. Mol. Pharmacol. **44**, 1192-201

FIGURE LEGENDS

Figure 1: **Expression of excitation-contraction coupling associated proteins in HMCL-7304-derived myotubes. A.** qPCR showing the relative expression levels of the indicated transcripts in HMCL-7304-derived myotubes compared to that in mature muscle biopsies. Expression levels were normalized for desmin content and are expressed as relative transcript content in biopsy/HMCL-7304-derived myotubes. The results are represented as Whisker plots performed on 4-5 controls and on the mytoube cell line. ***P<0.0001; **P< 0.07 and *P<0.003 by the Student's *t* test. **B.** Immunofluorescence of HMCL-7304-derived myotubes stained with anti- fast and slow myosin and DAPI and observed with a Leica DMR fluorescence microscope with a 20× objective. Scale bar = 50 μm. **C.** Western Blot analysis of RyR1 and CASQ2 (70 μg/lane), $Ca_V1.1$, SERCA1, SERCA2, MYH1- myosin heavy chain (50μg/lane). Blots were prepared and developed as detailed in the Methods section; for RyR1 the commercial monoclonal Antibodies 34C as well as the isoform 1 specific RyR polyclonal Antibodies (a kind gift of Prof. Vincenzo Sorrentino) recognize the same high molecular weight band corresponding to the RyR. Thus the lower less intense immunopositive band probably represents a proteolytic product. * indicates CSQ2.

Figure 2: Cellular localization of RyR1 and $Ca_v1.1$ in differentiated myotubes versus mouse FDB fibers by SIM microscopy. Human myotubes (A-F) and mouse FDB fibers (G-I) were stained with anti-$Ca_v1.1$ (A,D,G) and anti-RyR1 (B,E and H) antibodies and examined using Zeiss Elyra / ZEN 2010 microscope with a Plan-Apochromat 63x/1.4 Oil 3 rotations. Scale bar panels C and I = 5μm; scale bar panel F = 2 μm. Panels D, E and F are higher magnifications of the boxed areas shown in panels A, B and C, respectively. Double arrows in panel D represent nascent T-tubules; arrowheads in panel F show co-localization of RyR1 and $C_av1.1$.

Figure 3: Characterization of RyR1-mediated Ca^{2+} release in HMCL-7304-derived myotubes. Myotubes were loaded with 5μM of Fluo-4 and ,Ca^{2+} release from intercellular stores was measured in Krebs Ringer containing no added Ca^{2+} plus 100 μM La^{3+} as described in the Methods section. **A.** Photomicrograph of a fully differentiated myotube 5 days after differentiation (scale bar = 100 μm) **B.** Representative Ca^{2+} transient elicited by the addition of KCl; empty line above trace indicates Krebs Ringer containing 100 μM La^{3+}; filled line, stimulation with 60 mM KCl in 100 μM La^{3+}. Images were acquired every 100 msec with an electron multiplier Hamamatsu CCD C9100-13 camera and data was analyzed using Metamorph imaging software (Molecular Devices). **C.** Peak Ca^{2+} transients induced by 60 mM KCl, 10 mM Caffeine and 600 μM 4chloro-m-cresol; bar histograms represent the mean ± SEM ΔF (peak fluorescence –resting fluorescence) of 15 measurements. **D-F.** Dose response curves to caffeine, 4-chloro-m-cresol and KCl. Each point represents the mean (± SEM) ΔF of at least 10 different myotubes. The data were fitted using a Boltzmann equation using Origin 6.0 software.

Figure 4: **Skeletal L-type Ca^{2+} currents in HMCL-7304. A.** Whole-cell patch clamp recordings of single HMCL-7304 myotubes: cells were stimulated from a holding potential of –80 mV and a pre-step to –40 mV to increasing depolarizing potentials (see stimulation protocol). Membrane currents (sk I_{CaL}) were recorded in control solution (black trace) and during inhibition of I_{CaL} with $CdCl_2$ (500 μM, red trace). Original current traces and calculated difference current (ΔI_{CaL}, blue trace) are shown. **B.** Current-voltage relationship of sk I_{CaL} reveals a half maximal current activation at –9 ± 0.3 mV.

Figure 5: **Depolarization-induced Ca^{2+} release in HMCL-7304 myotubes. A.** Patch-clamped HMCL-7304 myotube loaded with fluo-3: the area of the linescan recording is indicated. Stimulation protocol, current response, line profile and linescan image of the Ca^{2+} transient are displayed in their respective temporal relation. **B.** Stimulation protocol and line profile of the resulting Ca^{2+} transients in a single protocol reveals the increase in Ca^{2+} release upon increasing membrane depolarization. **C.** Voltage-dependence of Ca^{2+} release: Peak Ca^{2+} transient amplitudes have been extracted and plotted in function of the stimulation potential. Half maximal Ca^{2+} release amplitude is achieved at -32 ± 2 mV.

Figure 1

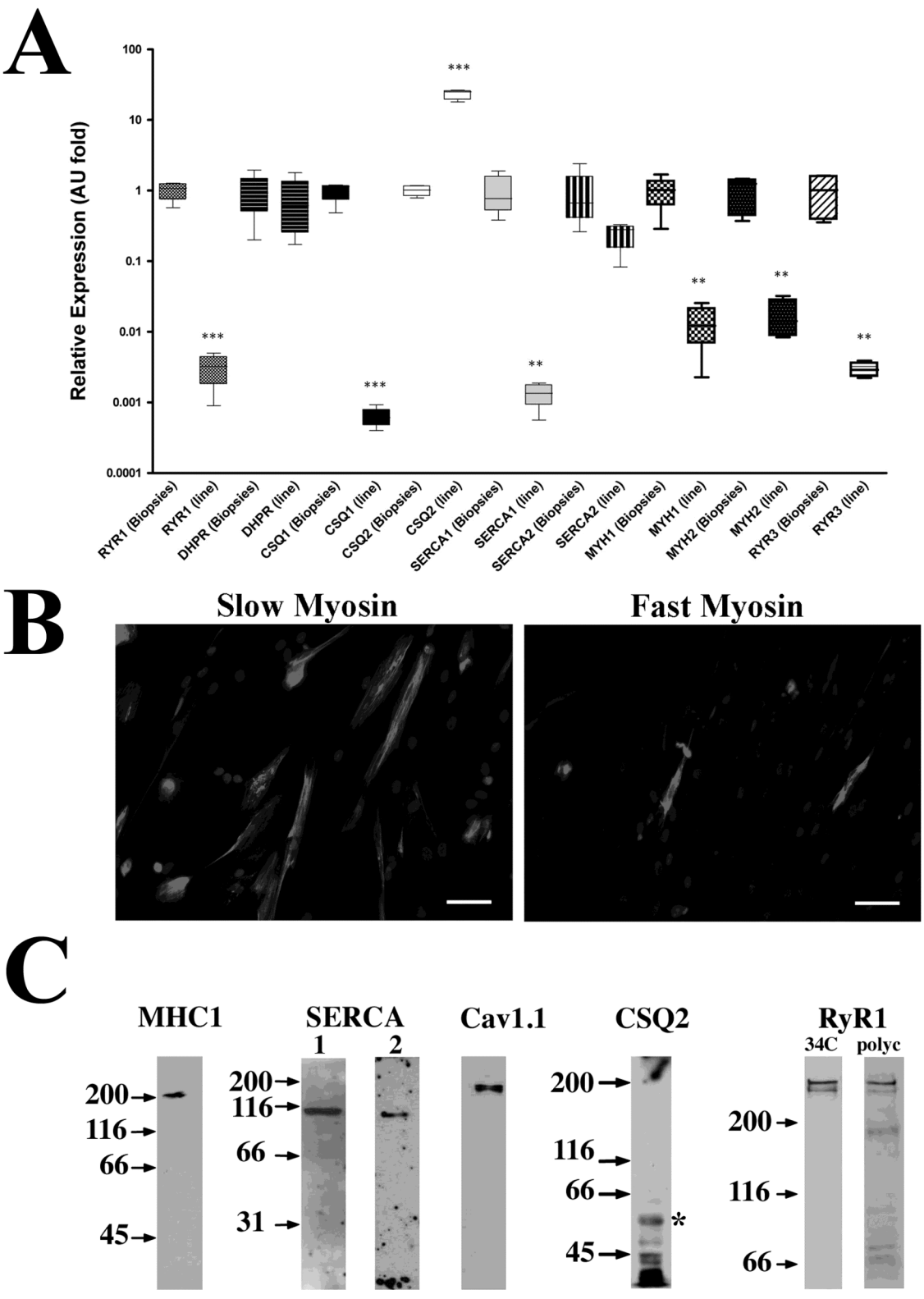
A
Relative Expression (AU fold)
100
10
1
0.1
0.01
0.001
0.0001
***
***
***
**
**
**
**
RYR1 (Biopsies)
RYR1 (line)
DHPR (Biopsies)
DHPR (line)
CSQ1 (Biopsies)
CSQ1 (line)
CSQ2 (Biopsies)
CSQ2 (line)
SERCA1 (Biopsies)
SERCA1 (line)
SERCA2 (Biopsies)
SERCA2 (line)
MYH1 (Biopsies)
MYH1 (line)
MYH2 (Biopsies)
MYH2 (line)
RYR3 (Biopsies)
RYR3 (line)
B
Slow Myosin
Fast Myosin
C
MHC1
SERCA
1
2
Cav1.1
CSQ2
RyR1
34C
polyc
200
116
66
45
31
*

Figure 2

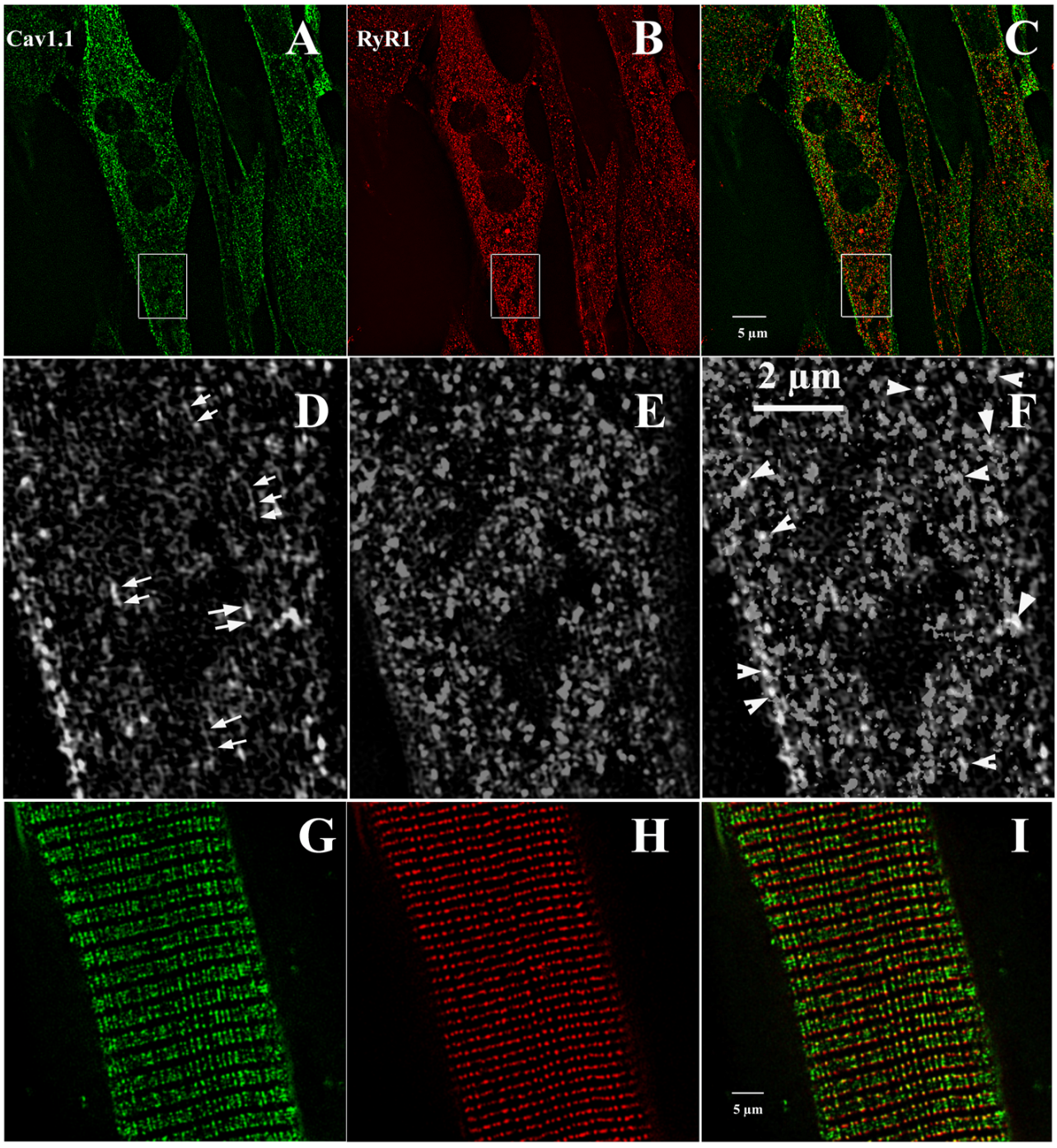

Figure 3

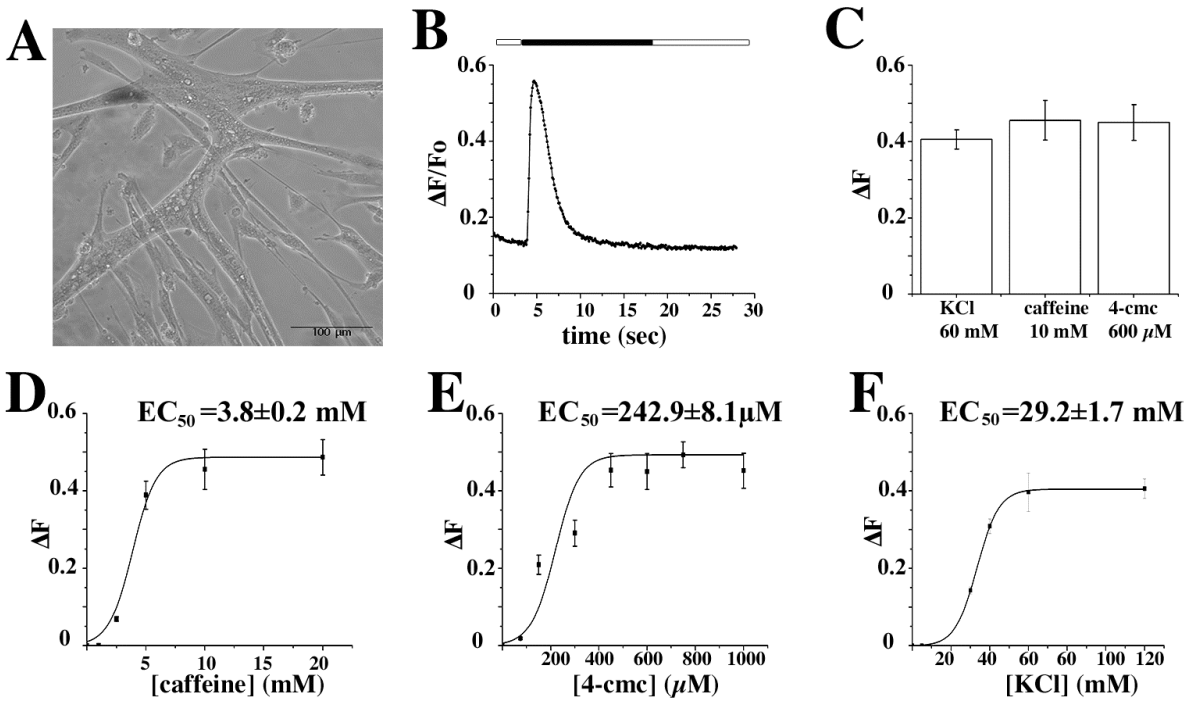
A
100 μm
B
ΔF/Fo
time (sec)
C
ΔF
KCl 60 mM
caffeine 10 mM
4-cmc 600 μM
D
EC50=3.8±0.2 mM
ΔF
[caffeine] (mM)
E
EC50=242.9±8.1μM
ΔF
[4-cmc] (μM)
F
EC50=29.2±1.7 mM
ΔF
[KCl] (mM)

Figure 4

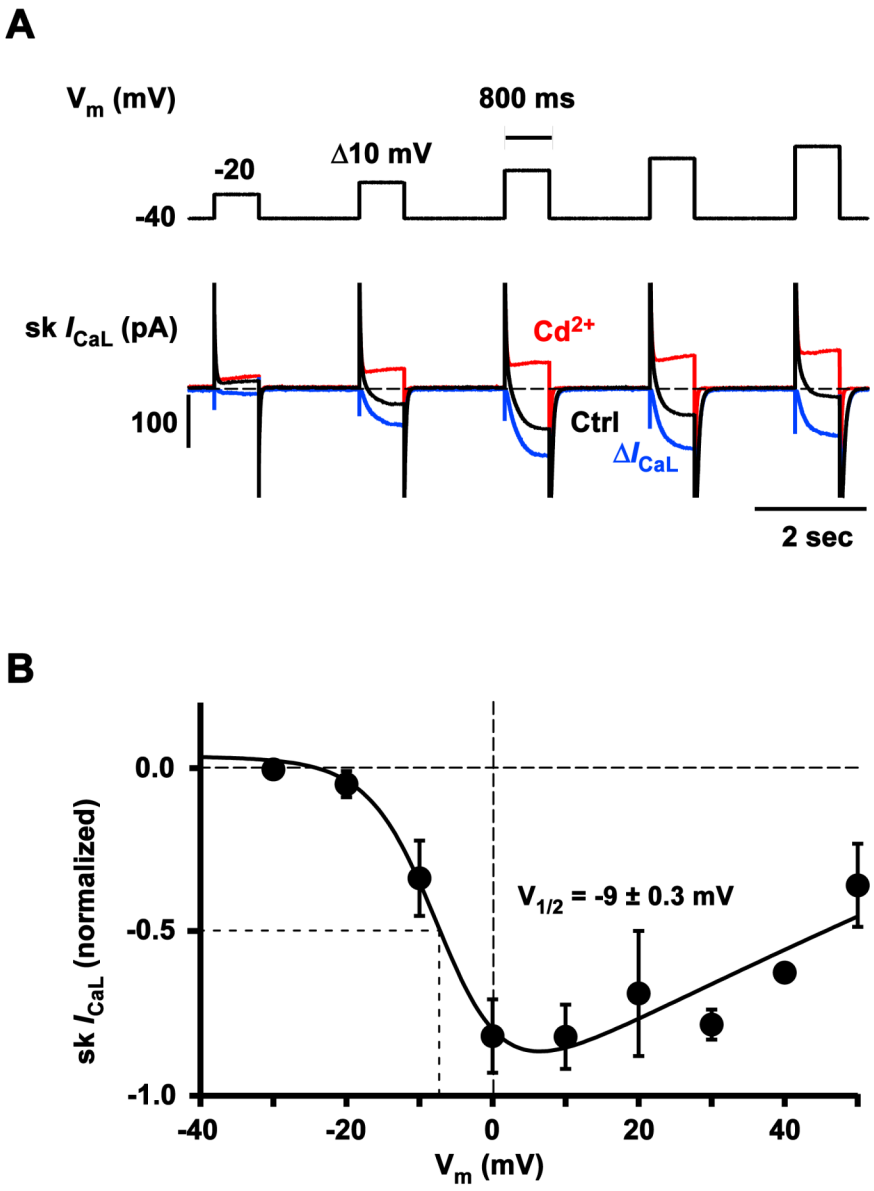
A
V_m (mV)
800 ms
-20
Δ10 mV
-40
sk I_{CaL} (pA)
Cd^{2+}
100
Ctrl
ΔI_{CaL}
2 sec
B
0.0
-0.5
-1.0
sk I_{CaL} (normalized)
$V_{1/2}$ = -9 ± 0.3 mV
-40
-20
0
20
40
V_m (mV)

Figure 5

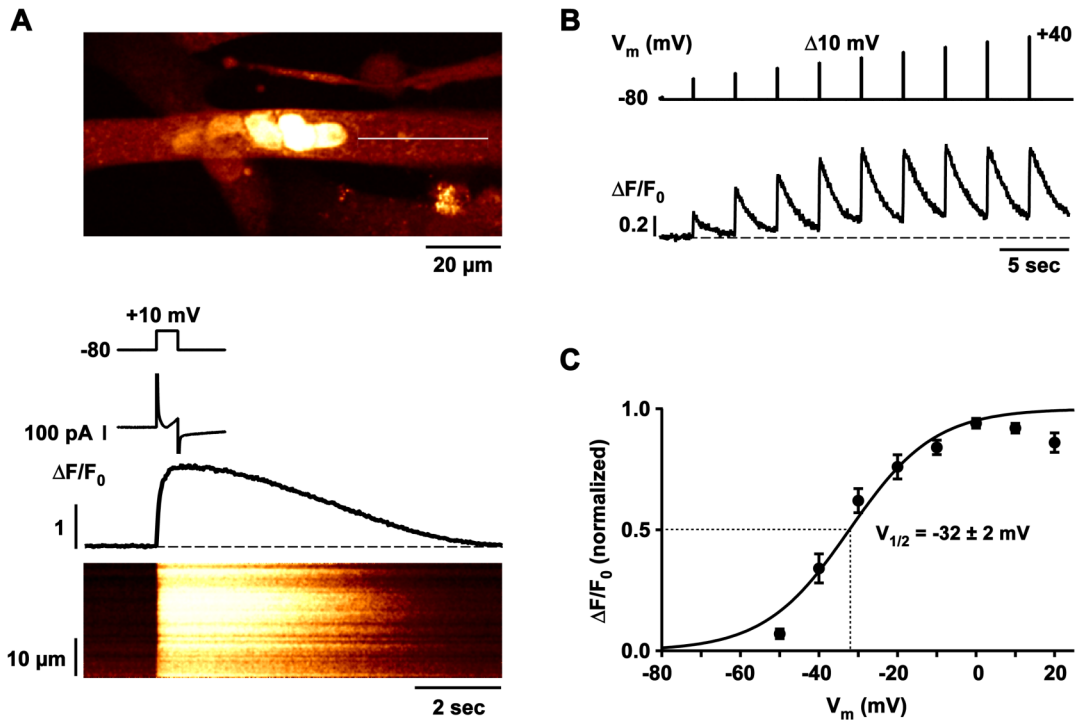
A
20 µm
+10 mV
-80
100 pA
ΔF/F0
1
10 µm
2 sec
B
Vm (mV)
Δ10 mV
+40
-80
ΔF/F0
0.2
5 sec
C
ΔF/F0 (normalized)
1.0
0.5
0.0
V1/2 = -32 ± 2 mV
-80
-60
-40
-20
0
20
Vm (mV)